

# High-Pressure Raman Studies on Aqueous Protonated Thiazole: Presence of Charge-Enhanced C–H···O Hydrogen Bonds

Hai-Chou Chang<sup>\*,†</sup>, Jyh-Chiang Jiang<sup>‡</sup>, Wen-Wei Lai,<sup>†</sup> Jui-San Lin,<sup>†</sup> Guan-Ciao Chen,<sup>†</sup> Wei-Cheng Tsai,<sup>†</sup> and Sheng Hsien Lin<sup>§,||</sup>

Department of Chemistry, National Dong Hwa University, Shoufeng, Hualien 974, Taiwan, Department of Chemical Engineering, National Taiwan University of Science and Technology, Taipei 106, Taiwan, Institute of Atomic and Molecular Sciences, Academia Sinica, P.O. Box 23-166, Taipei 106, Taiwan, and Department of Chemistry, National Taiwan University, Taipei 106, Taiwan

Received: July 5, 2005; In Final Form: October 7, 2005

Close interactions of the charge-enhanced C–H···O type have been analyzed both experimentally and computationally in the protonated thiazole–water system. The formation of a weak hydrogen bond was directly evidenced by a low-frequency shift of the hydrogen-bonded aromatic C–H stretch in the protonated thiazole moiety. For pure thiazole, the pressure dependence of the C–H bands yielded blue frequency shifts. The peak frequency of the aromatic C–H stretch band of protonated thiazole in a dilute D<sub>2</sub>O solution possesses an unusual nonmonotonic pressure dependence, which indicates enhanced C–H···O hydrogen-bond formation at high pressure. We performed density functional theory calculations to predict the frequency shift of the C–H stretching vibrations. The reorganization of the hydrogen-bonded network may be one of the factors to induce the blue frequency shift to the red frequency shift.

## Introduction

Weak hydrogen bonds, such as those between carbon and oxygen atoms (C–H···O), have received much attention of scientists owing to their many interesting and useful characteristics.<sup>1–4</sup> Various studies have been made to elucidate the role of C–H···O and C–H···X interactions in the structure of ionic liquids.<sup>5–8</sup> Nevertheless, experimental evidences of C–H···O hydrogen bonds are notoriously difficult to obtain, mainly because the C–H···O interactions usually coexist with other strong hydrogen bonds making the contribution from C–H···O interactions difficult to be distinguished, whereas the results of crystal structures are highly informative on the relative geometry changes, crystallography is silent on the question of whether C–H···O interactions are attractive or appear merely as a result of steric constraints.<sup>1,9</sup> Thus, the observation of the C–H stretching vibration is one of keys to characterize the presence of such a weak hydrogen bond and to evaluate the strength of the bond.

One of the intriguing aspects of weak hydrogen bonds is that the C–H covalent bond tends to shorten as a result of formation of a hydrogen bond with a Lewis base. Associated with this contraction is a shift of the C–H stretching frequency to the blue, as compared to the usual expectation of a red shift. Two schools of thought have emerged in trying to explain the physical basis for blue-shifted C–H frequencies.<sup>2,3,10</sup> As suggested by Hobza et al., the blue-shifting C–H···O may be attributed to the electron density transfer from the proton acceptor to the remote part of the proton donor.<sup>2</sup> Therefore, the blue-shifting C–H···O interactions were labeled as anti-hydrogen bonds.

However, Scheiner<sup>3</sup> and Dannenberg<sup>10</sup> et al. have concluded, from a set of theoretical calculations, that anti-hydrogen bonds do not differ fundamentally from conventional hydrogen bonds. According to their results, the electron density redistribution upon hydrogen-bond formation is similar for both the C–H···O and the O–H···O interactions. The amount of charge transferred from a donor to an acceptor is roughly proportional to the binding strength. One of the underlying reasons for this controversy is the weakness of C–H···O interactions. Therefore, the study of methods that enhance C–H···O interactions is crucial if we are to obtain a clear and unified view of this important phenomenon. Several studies have shown the potential significant effect that pressure has on controlling the strength of C–H···O interactions.<sup>8,11–15</sup> Strengths of the C–H···O interactions can also be enhanced in molecular aggregates containing charges.<sup>8,11,12</sup>

Recently, the possibility of C–H···O hydrogen bonds contributing to the stability of biological macromolecules has been under debate.<sup>16–18</sup> Arbely and Arkin<sup>17</sup> used an empirical correlation between vibrational frequency shifts and interaction energy and estimated an energy of –0.88 kcal/mol for the C–H···O hydrogen bond. Yohannan et al.<sup>16</sup> estimated the contribution of the C–H···O hydrogen bond to the stability of bR by mutating Thr24 to Ala, Val, and Ser. They suggested that this C–H···O hydrogen bond does not stabilize the protein. In this study, we present a novel means of looking at this controversy, by using variable pressure as a window into the nature of charge enhanced C–H···O interactions.

Thiazole is an important parent species, and its derivatives include thiamine (Vitamin B1) and the penicillins.<sup>19,20</sup> Because of the considerable  $\pi$ -electron delocalization, thiazole can be regarded as an aromatic molecule.<sup>19,20</sup> Four 2P<sub>z</sub> orbitals and one 3P<sub>z</sub> orbital form delocalized  $\pi$  molecular orbitals to which the three C atoms and the N atom each contribute one electron and the S atom contributes two electrons. The aromatic character

\* To whom correspondence should be addressed. E-mail: hcchang@mail.ndhu.edu.tw. Fax: +886-3-8633570. Phone: +886-3-8633585.

<sup>†</sup> National Dong Hwa University.

<sup>‡</sup> National Taiwan University of Science and Technology.

<sup>§</sup> Institute of Atomic and Molecular Sciences.

<sup>||</sup> National Taiwan University.

of thiazole is shown by the occurrence of a diamagnetic current induced in the ring during NMR experiments.<sup>19</sup> In the past, a great deal of effort has been made to understand the nature of aromatic C—H···O hydrogen bonds.<sup>21–24</sup> For the investigation of such a weak aromatic C—H···O hydrogen bond, vibrational spectroscopy is one of the most powerful techniques. The aromatic C—H stretch region in the infrared spectra is usually congested due to Fermi resonance. Thus, clear experimental evidences for aromatic C—H···O hydrogen bonds are difficult to obtain. In our current investigation, we used pressure as a variable to extract the hydrophobic structural information of aqueous protonated thiazole solutions and to alter the noncovalent aromatic C—H···O interactions from weak types to hydrogen-bond-like types.

The use of pressure as a variable allows one to change, in a controlled way, the intermolecular interactions without encountering the major perturbations produced by changes in temperature and chemical composition.<sup>25,26</sup> Static pressures up to several megabars can be generated using diamond anvil cells. The static approach is of interest because it allows continuous tuning of the pressure and the possibility to employ a large number of probing techniques that allow in situ measurements. Under high-pressure conditions, the relative weights of the strong intramolecular interactions responsible for molecular bonding, and of the weaker intermolecular forces defining the aggregation state, are altered, and the repulsive side of the intermolecular potential is explored. Nevertheless, the pressures used to investigate chemical systems typically range from ambient to several GPa.<sup>26</sup> Such pressures mainly change intermolecular distances and affect conformations. In the results and discussion section, we show that the combination of high pressure and Raman technique is sensitive method to probe the charge-enhanced hydrophobic structures in aqueous protonated thiazole.

## Experimental Section

Samples of binary mixtures were prepared using thiazole (>99%), supplied by Aldrich, and 99.97% D<sub>2</sub>O, supplied by Merck. The pH value was adjusted by adding 35% DCl solution. A diamond anvil cell (DAC) of Merrill–Bassett design, having a diamond culet size of 0.6 mm, was used for generating pressures up to ca. 3 GPa. Two type-Ia diamonds were used for Raman measurements. The sample was contained in a 0.3-mm-diameter hole in a 0.25-mm-thick stainless steel gasket mounted on the diamond anvil cell. A droplet of a sample filled the empty space of the entire hole of the gasket in the DAC, which was subsequently sealed when the opposed anvils were pushed toward one another.

The Raman spectra were measured using a 100 mw DPSS laser ( $\lambda = 532$  nm) and a home-built microscope-based Raman spectrometer with a 300-mm spectrograph (Acton SP308), equipped with an 1200 gr/mm holographic grating and a side window photon counting detector system. We chose 100  $\mu$ m slit width corresponding to a resolution of  $\sim 5$   $\text{cm}^{-1}$ .

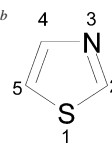
## Results and Discussion

We performed density functional theory calculations using the Gaussian 98 program package;<sup>27</sup> Table 1 displays the predicted C—H stretching frequencies of the thiazole monomer. Harmonic vibrational frequencies were obtained from analytical second derivatives at the B3LYP/6-31+G\* level and were scaled with a single factor (0.955).<sup>16–18</sup> Figure 1 presents Raman spectra of pure thiazole obtained under ambient pressure (curve a) and at 0.3 (curve b), 0.9 (curve c), 1.5 (curve d), 1.9 (curve e), 2.3 (curve f), and 2.5 GPa (curve g). The C—H stretching

**TABLE 1: DFT-Calculated C—H Stretching Frequencies ( $\text{cm}^{-1}$ ) and Raman Intensity ( $\text{km/mole}$ ) of Thiazole Monomer<sup>a,b</sup>**

calcd frequency (intensity)	assignment
3133 (130)	sym C(4,5)—H stretch
3103 (110)	C(2)—H stretch
3094 (106)	asym C(4,5)—H stretch

<sup>a</sup> Frequencies scaled by 0.955. <sup>b</sup>



e), 2.3 (curve f), and 2.5 GPa (curve g). As indicated in Figure 1a, the Raman spectrum of pure thiazole exhibits two bands at 3099 and 3130  $\text{cm}^{-1}$  corresponding to C—H stretching modes. A phase transition, i.e., pressure-induced solidification, was observed in Figure 1b, as the Raman spectrum of C—H stretching modes becomes three separated bands locating at 3091, 3106, and 3139  $\text{cm}^{-1}$ . A further increase in pressure leads to a blue frequency shift of all three C—H bands (i.e., in parts b–g of Figure 1). The blue shift may originate from the overlap repulsion effect enhanced by hydrostatic pressure. Analyzing the pressure dependence of the C—H stretches at ca. 3106 and 3139  $\text{cm}^{-1}$  yielded blue frequency shifts of ca. 11.0 and 6.6  $\text{cm}^{-1}/\text{GPa}$ , respectively. The pressure-induced frequency shift of the C(2)—H mode, i.e., the ca. 3106  $\text{cm}^{-1}$  band, are relatively large. This behavior may suggest the presence in the solid state of intermolecular C—H···N association involving the C(2)—H vibration which corresponds to the ca. 3106  $\text{cm}^{-1}$  band. Our results indicated that the pressure-enhanced C—H···N interactions may be a compensatory mechanism to provide additional stability. A study of hydrogen bonding between the thiazole rings and amide bonds showed that C—H···O hydrogen bonds were formed between thiazole and carbonyl O atoms in a  $\beta$ -sheet structure.<sup>23</sup> However, much more effort needs to be exerted to illustrate the nature of blue-shifting C—H bonds.

Figure 2 displays Raman spectra of a protonated thiazole/D<sub>2</sub>O mixture having its mole fraction of protonated thiazole equal to 0.3 (pH 1.4) obtained under ambient pressure (curve a) and at 0.3 (curve b), 0.9 (curve c), 1.5 (curve d), 1.9 (curve e), 2.3 (curve f), and 2.5 GPa (curve g). The C—H stretching overlaps with the O—H stretching bands of H<sub>2</sub>O, so we studied

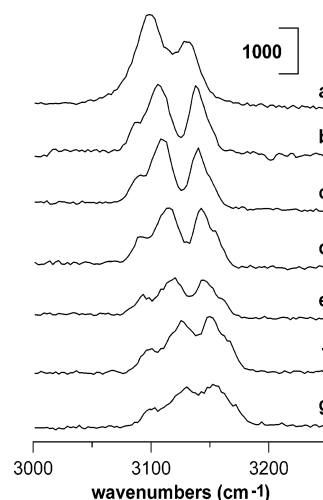


**Figure 1.** Raman spectra displaying the C—H stretching region of pure thiazole under (a) ambient pressure and at (b) 0.3, (c) 0.9, (d) 1.5, (e) 1.9, (f) 2.3, and (g) 2.5 GPa. The Raman intensity (counts) was labeled on the top right corner.

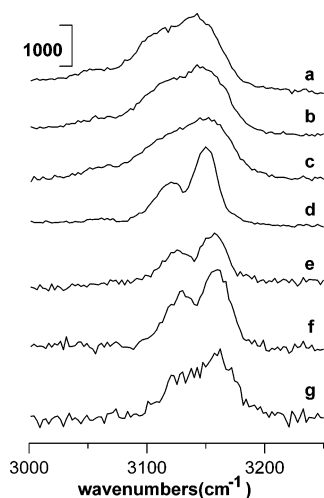
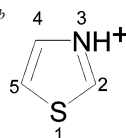


**Figure 2.** Pressure dependence of the Raman spectra in the C–H stretching region of a protonated thiazole/D<sub>2</sub>O mixture having its mole fraction of protonated thiazole equal to 0.3 (pH 1.4) under the following pressures: (a) ambient, (b) 0.3 GPa, (c) 0.9 GPa, (d) 1.5 GPa, (e) 1.9 GPa, (f) 2.3 GPa, and (g) 2.5 GPa.

**TABLE 2: DFT-Calculated C–H Stretching Frequencies (cm<sup>-1</sup>) and Raman Intensity (km/mole) of Protonated Thiazole Monomer<sup>a,b</sup>**

calcd frequency (intensity)	assignment
3147 (138)	sym C(4,5)–H stretch
3136 (52)	C(2)–H stretch
3132 (63)	asym C(4,5)–H stretch

<sup>a</sup> Frequencies scaled by 0.955. <sup>b</sup>



C–H stretching vibrations in a solution of D<sub>2</sub>O. The  $pK_a$  of thiazole is 2.52.<sup>19</sup> Thus, a thiazole solution of pH 1.4 is ca. 93% protonated thiazole. Table 2 displays the predicted C–H stretching frequencies of the protonated thiazole monomer using the Gaussian 98 program package.<sup>27</sup> As revealed in Figure 2a, the spectrum of protonated thiazole shows a strong C–H band at ca. 3145 cm<sup>-1</sup> and a shoulder at ca. 3115 cm<sup>-1</sup>. As the mixture was compressed, i.e., increasing the pressure from ambient (Figure 2a) to 0.9 GPa (Figure 2c), the blueshift in frequency was observed for the strong C–H band at ca. 3145 cm<sup>-1</sup>. We noticed, however, that no appreciable changes in band frequency of the prominent C–H stretching band occurred upon further compression (parts c and d of Figure 2). It is known that liquid water transforms at around 1 GPa to tetragonal ice VI and at around 2 GPa to cubic ice VII.<sup>28,29</sup> As the high-pressure ices are formed, some reorganization of the hydrogen-bonded network is expected.<sup>28–30</sup> Thus this discontinuity in frequency shift in Figure 2 may arise from the change of geometric properties of the hydrogen-bond network.

Figure 3 displays Raman spectra of a protonated thiazole/D<sub>2</sub>O mixture having its mole fraction of protonated thiazole equal to 0.1 (pH 0.8) obtained under ambient pressure (curve a) and at 0.3 (curve b), 0.9 (curve c), 1.5 (curve d), 1.9 (curve e), 2.3 (curve f), and 2.5 GPa (curve g). Analysis of the pressure dependence of the C–H peaks yields blue frequency shifts at pressure below 0.9 GPa (parts a–c of Figure 3), but a further increase in pressure leads to a red frequency shift of the dominant C–H band (Figure 3d). Both hydrogen-bond cooperative and geometric effects may be attributed the red frequency shift in Figure 3d. The reorganization of hydrogen-bonded

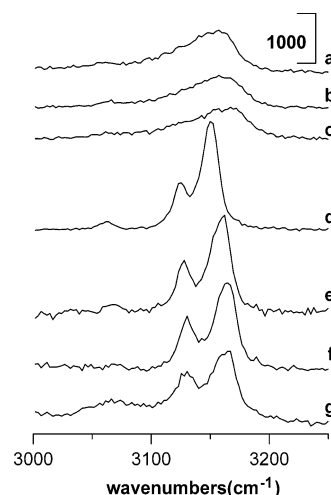


**Figure 3.** Pressure dependence of the Raman spectra displaying the C–H stretching region of a protonated thiazole/D<sub>2</sub>O mixture with mole fraction of protonated thiazole equal to 0.1 (pH 0.8) under the following pressures: (a) ambient, (b) 0.3 GPa, (c) 0.9 GPa, (d) 1.5 GPa, (e) 1.9 GPa, (f) 2.3 GPa, and (g) 2.5 GPa.

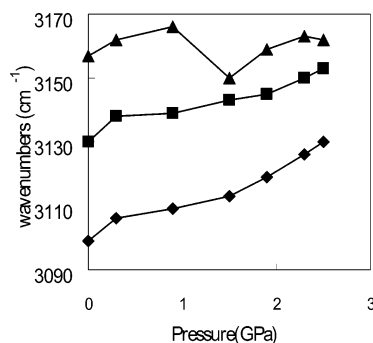


**Figure 4.** The C–H stretching frequency of protonated thiazole/D<sub>2</sub>O (triangle) and pure thiazole (square and diamond) vs the pressure.

network or geometry may be one of the factors to induce the blue frequency shift to the red frequency shift, as the high-pressure ices are formed. It is known that the hydrogen-bond cooperativity due to concerted charge transfer can greatly enhance the strength of the individual hydrogen bonds involving in the coupling. As the number of water molecules increases, the strength of C–H...O is augmented due to the concerted coupling. In the past, several models have been proposed for the theoretical understanding of the C–H...O interactions.<sup>1–4</sup> For example, when a molecule that is capable of forming blue-shifting hydrogen bonding binds to a site with a sufficiently strong electrostatic field to dominate over the overlap effect, that molecule is predicted to display a red-shifting hydrogen bond.<sup>10</sup> In this article, we present a means of looking at this issue by employing the high-pressure method.

To illustrate the frequency-shift, the pressure dependence of the C–H band frequencies of protonated thiazole (mole fraction 0.1, pH 0.8) and pure thiazole was plotted (Figure 4). As revealed in Figure 4, the pressure dependence of the C–H stretch of pure thiazole (square and diamond) yielded monotonic blue frequency shifts that correspond to contraction of the C–H bonds. Analysis of the pressure dependence of the dominant C–H peaks of protonated thiazole (triangle) yields blue frequency shifts at pressure below 1 GPa, but the red shift in frequency of the C–H band is obvious upon further compression. The red frequency shift should arise from an enhancement of the strength of C–H...O interactions, that is, from C–H...O hydrogen bonding as the high-pressure ices are formed. We

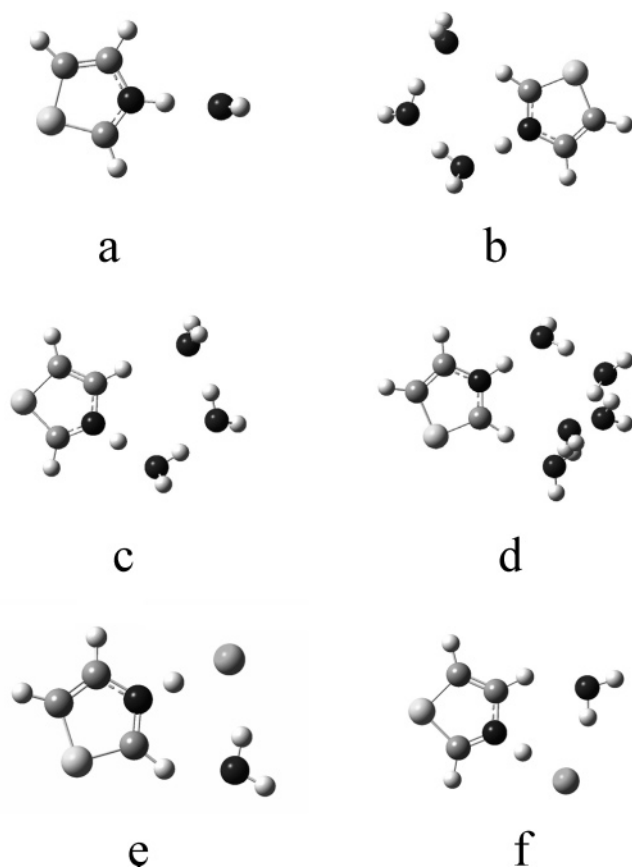


**Figure 5.** Optimized structures of (a) protonated thiazole-water, (b–c) protonated thiazole-(water)<sub>3</sub>, (d) protonated thiazole-(water)<sub>5</sub>, and (e–f) thiazole hydrochloride-(water).

note that the frequency of the C–H stretching modes that characterize the C–H···OD<sub>2</sub> hydrogen bonding ( $p > 1.5$  GPa) increases with increasing pressure. This behavior is in contrast with the general trend observed of a red shift with pressure for O–H and C=O stretching modes in strong hydrogen-bonded O–H···O and C=O···H system, respectively.<sup>28,29</sup> For donors such as O–H, the electrostatic component is the dominant one in a hydrogen bond, whereas for weakly polarized C–H groups the electrostatic component is of similar magnitude to the van der Waals contribution. Upon compression, the van der Waals contribution becomes repulsive and might even result in a blue shift in frequency; this will be more important the smaller the electrostatic component is.

Figure 5 displays the predicted structure of protonated thiazole-(water)<sub>*n*</sub> and thiazole hydrochloride-(water) clusters. The geometry optimization and vibrational frequencies of the clusters were calculated by using Becke3LYP level with 6-31+G\*.<sup>27</sup> As shown in Table 3, harmonic vibrational frequencies were obtained with a single scaling factor of 0.955. As illustrated in Figure 5a, the energetically favored approach for the water molecule to interact with the protonated thiazole ion is through the formation of N–H···O hydrogen bond. Figure 5b depicts the optimized geometry of protonated thiazole-(water)<sub>3</sub> with the participation of C(2)–H···O interactions. By comparison of parts a and b of Figure 5, we found that the C(2)–H band frequencies are red shifted by ca. 65 cm<sup>−1</sup>, as is indicated in Table 3. Figure 5c illustrates the optimized structure of protonated thiazole-(water)<sub>3</sub> with the participation of C(4)–H···O interactions. Figure 5c and Table 3 indicate the symmetric C(4,5)–H and asymmetric C(4,5)–H bands are shifted to lower frequencies at 3145 and 3096 cm<sup>−1</sup>, respectively. These calculation results, predicting the frequency red shift of the C–H

**TABLE 3: DFT-Calculated C–H Stretching Frequencies (cm<sup>−1</sup>) and Raman Intensity (km/mole) of Protonated Thiazole-(Water)<sub>*n*</sub> and Thiazole Hydrochloride-(Water)<sup>a,b</sup>**

species <sup>a</sup>	calcd frequencies (intensities) <sup>b</sup>	assignment
a	3148 (146), 3137 (52), 3133 (63)	sym C–H, C(2)–H, asym C–H
b	3148 (136), 3131 (67), 3072 (147)	sym C–H, asym C–H, b-C(2)–H
c	3145 (122), 3137 (58), 3096 (144)	sym C–H, C(2)–H, b-asym C–H
d	3149 (135), 3131 (68), 3029 (191)	sym C–H, asym C–H, b-C(2)–H
e	3146 (170), 3126 (64), 3041 (96)	sym C–H, asym C–H, b-C(2)–H
f	3143 (154), 3132 (54), 3074 (110)	sym C–H, C(2)–H, b-asym C–H

<sup>a</sup> Structures illustrated in Figure 5. <sup>b</sup> Frequencies scaled by 0.955.

vibrations, are consistent with our experimental observations in Figures 2–4. In other words, our results indicate charge-enhanced C–H···O hydrogen-bond formation at high pressure. As the clusters increase in size, the structural identification of the hydrophobic isomers is complicated by the presence of numerous different isomeric configurations. The questions of which clusters are responsible and how the weak hydrogen bond looks in detail may be settled by molecular dynamics, which is not the scope of this article. Figure 5d displays the structure of the protonated thiazole-(water)<sub>5</sub> that features C–H···O hydrogen bonding at the C(2)–H site. The characteristic bonded C(2)–H is redshifted in frequency to 3029 cm<sup>−1</sup> in Figure 5d. As revealed in parts a–c of Figure 3, the band at 3020–3080 cm<sup>−1</sup> is weak and broad under the pressure < 1 GPa. Increasing the pressure leads to the increase in intensity of the 3020–3080 cm<sup>−1</sup> band as seen in parts d–g of Figure 3. As high-pressure ices are formed, the size of hydrogen-bonded clusters in aqueous protonated thiazole may increase. Thus, the 3020–3080-cm<sup>−1</sup> band, being more obvious for low concentration of protonated thiazole under high pressure, may arise from the change of geometric properties of the hydrogen-bond network. It is instructive to note that the effect of chloride anion should not be excluded in this study.<sup>31</sup> Parts e and f of Figure 5 display the structures of thiazole hydrochloride-(water) with the participation of C(2)–H···O and C(4)–H···O, respectively. The low-energy bands at 3041 and 3074 cm<sup>−1</sup> are predicted in parts e and f of Figure 5, respectively. As shown in parts b and d of Figure 5 and Table 3, the C(2)–H stretching band is strongly red shifted when protonated thiazole is coordinated to three or five water molecules. This fact could be related to the well-known acidity of C(2)–H in 3-alkylthiazolium salts.<sup>19</sup> For example, deuteriodeprotonation of the C(2)-position in 3-alkylthiazolium salts by D<sub>2</sub>O can be catalyzed by bases such as triethylamine.<sup>19</sup>

The calculated changes in atomic charges, vibrational frequencies, and geometries relative to the protonated thiazole-water (for species b–d) and thiazole hydrochloride (for species e–f) are shown in Table 4. Table 4 indicates electron density loss from the bridging hydrogen atom as the results of C–H···O hydrogen-bond formation. It is known that the bridging proton becomes more positively charged, as the results of hydrogen-bond formation. This trend is characteristic of conventional hydrogen bonds as well as C–H···O hydrogen bonds.<sup>32</sup> As shown in Table 4, the bridging C–H bond elongations are accompanied by a red shift of the associated C–H stretching frequency. Importantly, the changes in Mulliken atomic charges of the C(2)–H bridging hydrogen (species b or e) are greater than those of the C(4)–H bridging hydrogen (species c or f). This observation indicates that C(2)–H is a



**TABLE 4: Changes in Mulliken Atomic Charge (me), Changes in C–H Stretching Frequencies (cm<sup>-1</sup>), Changes in CH Bond Lengths (Å), and CH...O Lengths Involving the Bridging Hydrogen**

species <sup>a</sup>	$\Delta Q$ (me)	$\Delta \nu$ (cm <sup>-1</sup> ) <sup>b</sup>	$\Delta r(\text{CH})$ (Å)	$\Delta(\text{CH}\cdots\text{O})$ (Å)
b	42	-65	0.0046	2.2589
c	37	-37	0.0030	2.4012
d	75	-108	0.0075	2.0703
e	125	-71	0.0064	2.0276
f	119	-31	0.0034	2.1089

<sup>a</sup> Structures illustrated in Figure 5. <sup>b</sup> Frequencies scaled by 0.955.**TABLE 5: Charge Transfer of Protonated Thiazole (me) and N–H Bond Lengths (Å)**

species <sup>a</sup>	charge transferred (me) <sup>b</sup>	$r(\text{N–H})$ (Å)
a	-35.8	1.0435
b	-69.3	1.0661
c	-68.1	1.0683
d	-40.9	1.0590

<sup>a</sup> Structures illustrated in Figure 5. <sup>b</sup> Calculated from the Mulliken charges of water clusters.

better proton donor than C(4)–H. As revealed in Table 5, there is a transfer of net charge that occurs between the protonated thiazole and water clusters upon formation of hydrogen-bonded complexes. The charge transfer of protonated thiazole was calculated from the Mulliken charges of water clusters. The electron density flows from the proton acceptor molecule to the donor, causing a greater negative charge on the latter and more positive charge on the former. In the cases of species b–d, there are two proton donors, i.e., one N–H and one C–H, on each protonated thiazole, but one cannot attribute the increased charge transfer of species b–d to one more particular C–H...O bond involved. In other words, the increased charge transfer in species b and c indicates the evidence of cooperativity. The lesser cooperativity for species d is caused by the orientation of the third water molecule from the N–H end. The trend of N–H bond lengths shown in Table 5 also supports our cooperativity arguments.

## Conclusions

In this article, we demonstrate that high pressure can be used to probe charge-enhanced C–H...O hydrogen bonds in aqueous protonated thiazole. For dilute aqueous protonated thiazole, the pressure dependence of the aromatic C–H stretch bands yielded blue frequency shifts at pressures below 0.9 GPa, but a further increase in pressure leads to a red frequency shift. The unusual pressure shifts may be relevant to pressure-enhanced C–H...O hydrogen bonding. The density functional theory calculations indicated that the reorganization of the hydrogen-bonded network may be one of the factors to induce the blue frequency shift to the red frequency shift. The charge-transfer effect was also evaluated.

**Acknowledgment.** The authors thank the National Dong Hwa University and the National Science Council (Contract No.

NSC 93-2113-M-259-004) of Taiwan for financial support. The authors thank Wen-Chi Chu for the assistance.

## References and Notes

- (1) Desiraju, G. R.; Steiner, T. *The Weak Hydrogen Bond*; Oxford: New York, 1999.
- (2) Hobza, P.; Havlas, Z. *Chem. Rev.* **2000**, *100*, 4253.
- (3) Gu, Y. L.; Kar, T.; Scheiner, S. *J. Am. Chem. Soc.* **1999**, *121*, 9411.
- (4) Wiczorek, R.; Dannenberg, J. J. *J. Am. Chem. Soc.* **2003**, *125*, 8124.
- (5) Del Popolo, M. G.; Lynden-Bell, R. M.; Kohanoff, J. *J. Phys. Chem. B* **2005**, *109*, 5895.
- (6) Mele, A.; Tran, C. D.; De Paoli Lacerda, S. H. *Angew. Chem., Int. Ed.* **2003**, *42*, 4364.
- (7) Hardacre, C.; Holbrey, J. D.; McMath, S. E. J.; Bowron, D. T.; Soper, A. K. *J. Chem. Phys.* **2003**, *118*, 273.
- (8) Lee, K. M.; Chang, H. C.; Jiang, J. C.; Lu, L. C.; Hsiao, C. J.; Lee, Y. T.; Lin, S. H.; Lin, I. J. B. *J. Chem. Phys.* **2004**, *120*, 8645.
- (9) Kang, B. S.; Devedjiev, Y.; Derewenda, U.; Derewenda, Z. S. *J. Mol. Biol.* **2004**, *338*, 483.
- (10) Masunov, A.; Dannenberg, J. J.; Contreras, R. H. *J. Phys. Chem. A* **2001**, *105*, 4737.
- (11) Chang, H. C.; Lee, K. M.; Jiang, J. C.; Lin, M. S.; Chen, J. S.; Lin, I. J. B.; Lin, S. H. *J. Chem. Phys.* **2002**, *117*, 1723.
- (12) Lee, K. M.; Chang, H. C.; Jiang, J. C.; Chen, J. C. C.; Kao, H. E.; Lin, S. H.; Lin, I. J. B. *J. Am. Chem. Soc.* **2003**, *125*, 12358.
- (13) Chang, H. C.; Jiang, J. C.; Su, C. C.; Lu, L. C.; Hsiao, C. J.; Chuang, C. W.; Lin, S. H. *J. Phys. Chem. A* **2004**, *108*, 11001.
- (14) Chang, H. C.; Jiang, J. C.; Chuang, C. W.; Lin, J. S.; Lai, W. W.; Yang, Y. C.; Lin, S. H. *Chem. Phys. Lett.* **2005**, *410*, 42.
- (15) Chang, H. C.; Jiang, J. C.; Chuang, C. W.; Lin, S. H. *Chem. Phys. Lett.* **2004**, *397*, 205.
- (16) Yohannan, S.; Faham, S.; Yang, D.; Grosfeld, D.; Chamberlain, A. K.; Bowie, T. U. *J. Am. Chem. Soc.* **2004**, *126*, 2284.
- (17) Arbely, E.; Arkin, I. T. *J. Am. Chem. Soc.* **2004**, *126*, 5362.
- (18) Mottamal, M.; Lazaridis, T. *Biochemistry* **2005**, *44*, 1607.
- (19) Eicher, T.; Hauptmann, S. *The Chemistry of Heterocycles*; Stuttgart: New York 1995.
- (20) Balaban, A. T.; Oniciu, D. C.; Katritzky, A. R. *Chem. Rev.* **2004**, *104*, 2777.
- (21) Montejo, M.; Navarro, A.; Kearley, G. J.; Vazquez, J.; Lopez-Gonzalez, J. J. *J. Am. Chem. Soc.* **2004**, *126*, 15087.
- (22) Sbrana, G.; Muniz-Miranda, M. *J. Phys. Chem. A* **1998**, *102*, 7602.
- (23) Asano, A.; Taniguchi, T.; Sasaki, M.; Hasegawa, H.; Katsuya, Y.; Doi, M. *Acta Crystallogr.* **2001**, *E57*, o834.
- (24) Venkatesan, V.; Fujii, A.; Ebata, T.; Mikami, N. *Chem. Phys. Lett.* **2004**, *394*, 45.
- (25) Bridgman, P. W. *Proc. Am. Acad. Arts Sci.* **1911**, *47*, 441.
- (26) Jonas, J.; Jonas, A. *Annu. Rev. Biophys. Struct.* **1994**, *23*, 287.
- (27) Frisch, M. J.; Trucks, G. W.; Schlegel, H. B.; Scuseria, G. E.; Robb, M. A.; Cheeseman, J. R.; Zakrzewski, V. G.; Montgomery, J. A., Jr.; Stratmann, R. E.; Burant, J. C.; Dapprich, S.; Millam, J. M.; Daniels, A. D.; Kudin, K. N.; Strain, M. C.; Farkas, O.; Tomasi, J.; Barone, V.; Cossi, M.; Cammi, R.; Mennucci, B.; Pomelli, C.; Adamo, C.; Clifford, S.; Ochterski, J.; Petersson, G. A.; Ayala, P. Y.; Cui, Q.; Morokuma, K.; Malick, D. K.; Rabuck, A. D.; Raghavachari, K.; Foresman, J. B.; Cioslowski, J.; Ortiz, J. V.; Baboul, A. G.; Stefanov, B. B.; Liu, G.; Liashenko, A.; Piskorz, P.; Komaromi, I.; Gomperts, R.; Martin, R. L.; Fox, D. J.; Keith, T.; Al-Laham, M. A.; Peng, C. Y.; Nanayakkara, A.; Gonzalez, C.; Challacombe, M.; Gill, P. M. W.; Johnson, B. G.; Chen, W.; Wong, M. W.; Andres, J. L.; Head-Gordon, M.; Replogle, E. S.; Pople, J. A. *Gaussian 98*, revision A.7; Gaussian Inc.: Pittsburgh, PA, 1998.
- (28) Franks, F. *Water, A Comprehensive Treatise*; Plenum: London, 1972; Vol. 1.
- (29) Chang, H. C.; Huang, K. H.; Yeh, Y. L.; Lin, S. H. *Chem. Phys. Lett.* **2000**, *326*, 93.
- (30) Chang, H. C.; Jiang, J. C.; Lin, S. H.; Weng, N. H.; Chao, M. C. *J. Chem. Phys.* **2001**, *115*, 3215.
- (31) Su, C. C.; Chang, H. C.; Jiang, J. C.; Wei, P. Y.; Lu, L. C.; Lin, S. H. *J. Chem. Phys.* **2003**, *119*, 10753.
- (32) Kar, T.; Scheiner, S. *J. Phys. Chem. A* **2004**, *108*, 9161.